Electronic Supplementary Material (ESI) for ChemComm.

Supporting Information for

Intramolecular H-bond Stabilization of a Primary Hydroxylamine in Salen-Type Metal Complexes

Hardeep Singh,[‡] Alyson MacKay,[‡] Nooshin Sheibany, Fei Chen, Maëlle Mosser, Pierre-Étienne Rouet, Frédéric Rousseau, Mohammad S. Askari and Xavier Ottenwaelder*

Department of Chemistry and Biochemistry, Concordia University, 7141 Sherbrooke Street West Montreal, Quebec, Canada, H4B 1R6

Email: dr.x@concordia.ca

1. Experimental Procedures

1.1 Materials

Organic reagents, solvents and metal salts for synthesis were commercially available reagent grade and used as received. For oxidation reactions, non-protic solvents were dried on an MBraun solvent purification system and stored over activated 4 Å molecular sieves inside an MBraun inert-atmosphere (N_2) glovebox filled with a dry nitrogen atmosphere (O_2 < 0.1 ppm; H_2O < 0.1 ppm). Air-sensitive samples were also stored in the glovebox. Oxidation experiments were carried out in a Radleys® carousel reaction station attached to O_2 tank.

1.2 Characterization Methods

^{1}H-NMR spectra were recorded in $CDCl_3$, DMSO-d_6 or acetone-d_6 at 25°C on a Varian Innova 500 MHz or Bruker Fourier 300 MHz and referenced to an internal standard of TMS (tetramethylsilane). Elemental analysies were carried out at the Laboratoire d'Analyse Élémentaire de l'Université de Montréal. Electrospray-ionization mass-spectrometry (ESI-MS) measurements were performed via direct injection on an Orbitrap LC-MS instrument at Concordia's Centre for Biological Applications of Mass Spectrometry. GC measurements were performed on an Agilent 6850 equipped with an HP-5 capillary column (5%-Phenyl)-methylpolysiloxane stationary phase, and an FID detector. Hexamethylbenzene was used as an internal standard for GC yield calculations.

1.3 X-Ray Crystallography

Crystallographic analysis was performed on a Bruker APEX-DUO diffractometer using the Cu-Kα or the Mo-Kα source. The frames were integrated with the Bruker SAINT software package using a narrow-frame algorithm. Data were corrected for absorption effects using the multiscan method (SADABS, or TWINABS in the case of twinned samples). The structures were solved by direct methods and refined using the APEX3 software package. All non-H atoms were refined with anisotropic thermal parameters. In some cases, restraints were used to solve disorder on portions of the molecules of interest or crystallization solvent molecules. In the best quality datasets, most H atoms could be identified on difference electronic map. Still, H atoms were generated in idealized positions, riding on the carrier atoms with isotropic thermal parameters.

1.4 Synthesis of Nitro Ligands

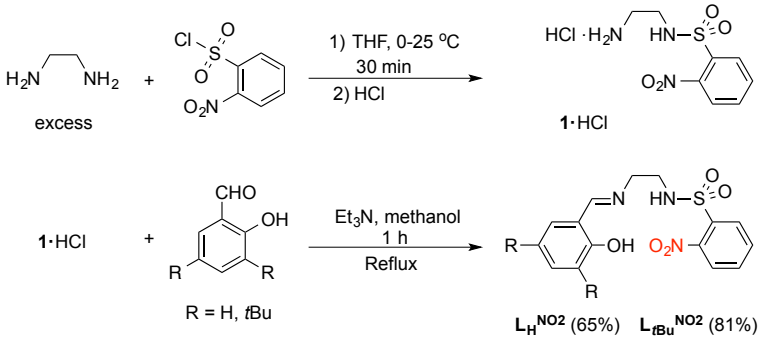

Scheme S1: Synthesis of $L_H^{NO_2}$ and $L_{tBu}^{NO_2}$.

1·HCl: This compound and the following were prepared by a previously reported method.[1] In a 250 mL round-bottom flask readied with a magnetic stir bar, ethylenediamine (10 mL, 8.94 g 148.75 mmol) was dissolved in anhydrous THF (25 mL) at 0°C followed by the dropwise addition of 2-nitrophenylsulfonyl chloride (10.98 g, 49.54 mmol) in anhydrous THF (50 mL). The solution was then warmed to room temperature, stirred for further 30 minutes, and then evaporated to dryness to give an oily residue, which was partitioned with dichloromethane (DCM, 50 mL) and water (50 mL). The aqueous layer was further extracted with 3 × 50 mL of DCM. The organics were combined, dried over Na_2SO_4, filtered, and the solvent was removed in vacuo to yield a brown oil. Concentrated HCl (50 mL, 12 M) was added to the oil, thereupon the bis(sulfonamide) by-product precipitated as a colourless solid. The solid was filtered off and the filtrate was concentrated to give a brown oil (mono-substituted ethylenediammonium salt, **1**·HCl) which was further used for the next steps without characterization.

$L_H^{NO_2}$:[1] In a 250 mL round-bottom flask, **1**·HCl was dissolved in methanol (50 mL). To this solution, salicylaldehyde (6.40 mL, 7.26 g, 59.45 mmol) and triethylamine (6.91 mL, 5.01 g, 49.54 mmol) were added under stirring. The solution was refluxed under stirring for 30 min, after which the stirring was stopped and the solution cooled to 25°C, then to 0°C. The yellow microcrystalline solid was filtered off and washed with cold methanol (50 mL). Yield: 11 g, 65% based on 2-nitrobenzenesulfonyl chloride. ^{1}H-NMR (500 MHz, $CDCl_3$, **Figure S1**) δ: 12.59 (s, 1H), 8.24 (s, 1H), 8.11 (dd, *J* = 7.8, 1.4 Hz, 1H), 7.68 (d, *J* = 8.0 Hz, 1H), 7.65 (d, *J* = 9.4 Hz, 1H), 7.58 (td, *J* = 7.7, 1.4 Hz, 1H), 7.29 (td, *J* = 7.8, 1.7 Hz, 1H), 7.14 (dd, *J* = 7.6, 1.7 Hz, 1H), 6.87 (dd, *J* = 9.5, 0.9 Hz, 1H), 6.84 (dd, *J* = 7.5, 1.0 Hz, 1H), 5.51 (s, 1H), 3.73 (td, *J* = 5.7, 1.0 Hz, 2H), 3.54 (td, *J* = 5.7, 1.0 Hz, 2H) ppm. Elemental analysis: calculated for $C_{15}H_{15}N_3O_5S$: C 51.57, H 4.33, N 12.03, S 9.18; found: C 51.67, H 4.11, N 12.06, S 9.24%.

$L_{tBu}^{NO_2}$: In a 250 mL round-bottom flask equipped with a stir bar, **1**·HCl was dissolved in methanol (50 mL) and to this solution, triethylamine (6.91 mL, 5.01 g, 49.54 mmol) and 3,5-di-*tert*-butylsalicyaldehyde[2] (13.930 g, 56.45 mmol) were added. After reflux under stirring for 1 h, stirring was stopped and the reaction mixture cooled down to 25°C, then to 0°C. The yellow microcrystalline solid was filtered off and washed with cold methanol (50 mL). Yield: 18.56 g, 81% based on 2-nitrobenzenesulfonyl chloride. A single-crystal was selected for X-ray diffraction analysis, which confirmed the molecular structure (**Figure S22**). ^{1}H-NMR (500 MHz, $CDCl_3$, **Figure S2**) δ: 13.01 (s, 1H), 8.24 (s, 1H), 8.14 (dd, *J* = 7.8, 1.2 Hz, 1H), 7.75 (dd, *J* = 7.9, 1.1 Hz, 1H), 7.67 (td, *J* = 7.7, 1.2 Hz, 1H), 7.60 (td, *J* = 7.8, 1.3 Hz, 1H), 7.38 (d, *J* = 2.4 Hz, 1H), 6.96 (d, *J* = 2.4 Hz, 1H), 5.54 (t, *J* = 5.9 Hz, 1H), 3.73 (td, *J* = 11.6, 5.9 Hz, 2H), 3.52 (td, *J* = 11.6, 5.9 Hz, 2H), 1.42 (s, 9H), 1.30 (s, 9H) ppm. Elemental analysis: calculated for $C_{23}H_{31}N_3O_5S$: C 59.85, H 6.77, N 9.10, S 6.95; found: C 59.82, H 6.88, N 9.17, S 6.90%.

1.5 Synthesis of Hydroxylamine Ligands

Table S1. Optimization of the hydrogenation conditions

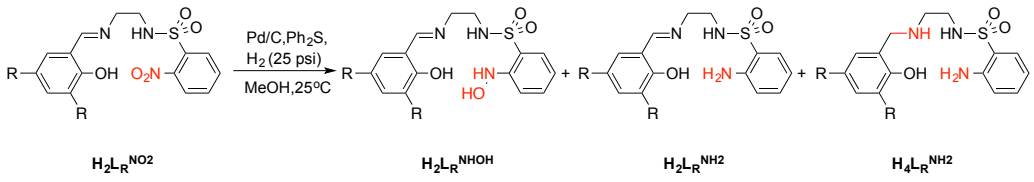

$H_2L_R^{NO2}$ $H_2L_R^{NHOH}$ $H_2L_R^{NH2}$ $H_4L_R^{NH2}$

Entry	R	Time (h)	Poison (%/Pd)	% compounds [b]			
				$H_2L_R^{NO_2}$	$H_2L_R^{NHOH}$	$H_2L_R^{NH_2}$	$H_4L_R^{NH_2}$
1	H	5	-	-	-	-	100
2	H	2	-	-	-	30	70
3	H	1	-	-	-	45	55
4	H	0.5	-	-	38	62	-
5	H	0.5	5	26	62	12	-
6	H	1	5	20	70	10	-
7	H	0.83	10	16	80	4	-
8	*t*Bu	1	10	13	84	3	-

[a] Pd/C (2 mol% Pd per substrate), Ph_2S (mol% per Pd), 25 psi H_2, MeOH, 25°C. [b] Quantities based on ^{1}H-NMR ratios.

Table S2. TLC R_f values and characteristic ^{1}H-NMR signals for the CH_2CH_2 backbone.

Ligand	R_f [a]	^{1}H-NMR signals [b]				Ligand	R_f [c]	^{1}H-NMR signals [b]			
$L_H^{NO_2}$	0.84	**3.73**	3.54			$L_{tBu}^{NO_2}$	0.66	**3.73**	3.53		
L_H^{NHOH}	0.47		3.55		**3.12**	L_{tBu}^{NHOH}	0.25		3.48		**3.18**
$L_H^{NH_2}$	0.56		3.58	**3.27**		$L_{tBu}^{NH_2}$	0.35		3.59	**3.26**	

[a] TLC on silica, DCM:MeOH 97:3. [b] $CDCl_3$, 25°C, 500MHz; values in ppm. In bold, the most characteristic signals, which were used for reaction optimization. [c] TLC on silica, DCM:MeOH 99:1.

L_H^{NHOH}: To a medium-pressure hydrogenation flask configured in a Parr shaker was added Pd/C (10 wt.% Pd) (30.4 mg, 0.0286 mmol) followed by slow addition of methanol (30 mL). Then, 100 µL of a 0.0286 M diphenyl sulfide[3] (0.533 mg, 0.00286 mmol) solution in methanol (5 mL) was added, followed by another 20 mL of methanol and $L_H^{NO_2}$ (500 mg, 1.43 mmol) dissolved in DCM (25 mL). The hydrogenation was carried out at 25 psi of H_2 at 25°C for 50 min. The catalyst was then filtered off over a pad of Celite, which was well rinsed with methanol (ca. 100 mL). After evaporating the filtrate to dryness, a minimum quantity of diethyl ether (ca. 9 mL) was added to the residue. The solid, which is the starting material, was filtered off and the filtrate was evaporated to dryness to give L_H^{NHOH} as a yellow powder. Yield: 434 mg, 91%. ^{1}H-NMR (500 MHz, $CDCl_3$, **Figure S3**) δ: 13.20 (br, 1H), 8.26 (s, 1H), 7.88 (dd, *J* = 7.7, 1.3 Hz, 1H), 7.64 (br, 1H), 7.55 (dd, *J* = 8.2, 1.3 Hz, 1H), 7.53-7.50 (m, 1H), 7.39-7.36 (m, 1H), 7.24 (dd, *J* = 7.6, 1.7 Hz, 1H), 7.07-7.04 (m, 1H), 6.98 (dd, *J* = 8.1, 1.0 Hz, 1H), 6.95 (td, *J* = 7.5, 1.1 Hz, 1H), 6.45 (s, 1H), 5.65 (s, 1H), 3.56-3.54 (m, 2H), 3.12 (m, 2H) ppm.

L_{tBu}^{NHOH}: In a medium-pressure hydrogenation flask mounted on a Parr shaker, Pd/C (10 wt.% Pd) (22.98 mg, 0.0216 mmol) was placed with slow addition of methanol (30 mL). To this mixture, 100 µL of a 0.0216 M diphenyl sulfide[3] (0.402 mg, 0.00216 mmol) solution in methanol (5 mL) was added, followed by another 20 mL of methanol and $L_{tBu}^{NO_2}$ (500 mg, 1.08 mmol) dissolved in DCM (25 mL). The hydrogenation was carried out at 25 psi of H_2 pressure at 25°C for 1 h. The work-up was the same as for L_H^{NHOH} to yield L_{tBu}^{NHOH} as a yellow powder. Yield: 459 mg, 95%. ^{1}H-NMR (500 MHz, $CDCl_3$, **Figure S4**) δ: 13.48 (br, 1H), 8.19 (s, 1H), 7.82 (d, *J* = 7.5 Hz, 1H), 7.69 (s, 1H), 7.53 (s, 1H), 7.53-7.52 (m, 1H), 7.44 (d, *J* = 2.4 Hz, 1H), 7.05 (d, *J* = 2.4 Hz, 1H), 7.02-7.09 (m, 1H), 6.10 (s, 1H), 5.71 (t, *J* = 5.9 Hz, 1H), 3.44 (m, 2H), 3.19 (md, *J* = 5.9 Hz, 2H), 1.45 (s, 9H), 1.30 (s, 9H) ppm.

1.6 Synthesis of Complexes

Scheme S2: General scheme for the complexation of imine NHOH (L^I_R-NHOH) ligands with Cu(II), Ni(II) and Zn(II).

L_H^{NHOH}Cu: To a stirring solution of L_H^{NHOH} (110 mg, 0.327 mmol) in ACN (5 mL), a solution of $Cu(OAc)_2 \cdot H_2O$ (65.4 mg, 0.327 mmol) in ACN (5 mL), was added dropwise. The mixture was stirred vigorously for 15 min, during which a green solid precipitated out. The solid was collected by filtration, washed with diethyl ether (20 mL) and dried under vacuum to give a dark green powder. Yield: 75 mg, 58 %. Crystals suitable for X-ray diffraction

analysis were obtained by subjecting a small portion of the complex dissolved in DCM to vapour-diffusion of pentane at room temperature.

L_{tBu}^{NHOH}Cu: To a stirring solution of $Cu(OAc)_2 \cdot H_2O$ (127.9 mg, 0.641 mmol) in ACN (5 mL), a solution of L_{tBu}^{NHOH} (287 mg, 0.641 mmol) in ACN (5 mL) was added dropwise. The mixture was stirred vigorously in air for 15 min, during which a purple solid precipitated out. The solid was collected by filtration, washed with diethyl ether (20 mL) and then dried under vacuum to give a purple powder. Crystals suitable for X-ray diffraction analysis were obtained by placing a small portion of copper(II) acetate dihydrate (13 mg, 0.0447 mmol) in a vial and then layering it with L_{tBu}^{NHOH} (30 mg 0.0447 mmol) dissolved in 5 mL of ACN inside an inert-atmosphere glovebox. The mixture was left standing in the –30°C freezer for 3 days to obtain purple crystals. Yield: 217 mg, 67%. Elemental analysis: calculated for $C_{23}H_{31}N_3O_4SCu$: C 54.26, H 6.14, N 8.25, S 6.30; found: C 54.26, H 6.18, N 8.24, S 6.21%.

L_H^{NHOH}Ni: To a stirring solution of $Ni(NO_3)_2 \cdot 6H_2O$ (216.6 mg, 0.75 mmol) in ACN (5 mL), a solution of L_H^{NHOH} (250 mg, 0.7454 mmol) in ACN (5 mL) was added dropwise. The mixture was stirred vigorously for 15 min, during which a green solid precipitated out. The solid was collected by filtration, washed with diethyl ether (20 mL) and then dried under vacuum to give a muddy-green powder. Yield: 215 mg, 74%. Crystals suitable for X-ray diffraction analysis were obtained by subjecting a small portion of the complex dissolved in DCM to vapour-diffusion of pentane at room temperature. ^{1}H-NMR (500 MHz, $CDCl_3$, **Figure S5**) δ: 8.93 (br, 1H), 8.39 (br, 1H), 7.76 (d, *J* = 8.0 Hz, 1H), 7.74 (dd, *J* = 7.5, 1.2 Hz, 1H), 7.57 (t, *J* = 7.9 Hz, 1H), 7.55 (br, 1H), 7.35 (t, *J* = 7.6 Hz, 1H), 7.29-7.27 (m, 1H), 7.19 (dd, *J* = 7.9, 1.6 Hz, 1H), 6.87 (d, *J* = 8.5 Hz, 1H), 6.70 (t, *J* = 7.1 Hz, 1H), 3.56 (br, 1H), 3.31 (br, 1H), 2.82 (br, 1H), 2.77 (br, 1H) ppm. ^{13}C-NMR (125 MHz, $CDCl_3$, **Figure S6**) δ: 167.4, 160.1, 147.5, 134.3, 133.1, 131.7, 128.8, 123.2, 120.9, 119.6, 118.4, 117.1, 114.9, 56.8, 44.2 ppm. Elemental analysis: calculated for $C_{15}H_{15}N_3O_4SNi$: C 45.95, H 3.83, N 10.72, S 8.18; found: C 45.83, H 3.73, N 10.74, S 8.55%.

L_{tBu}^{NHOH}Ni: To a stirring solution of $Ni(NO_3)_2 \cdot 6H_2O$ (33.7 mg, 0.116 mmol) in ACN (5 mL), a solution of L_{tBu}^{NHOH} (52 mg, 0.116 mmol) in ACN (5 mL) was added dropwise. The mixture was stirred vigorously in air for 15 min, during which a green solid precipitated out. The solid was collected by filtration, washed with diethyl ether (20 mL) and then dried under vacuum to give a light-green powder. Yield: 42 mg, 72%. Crystals suitable for X-ray diffraction analysis were obtained by subjecting a small portion of the complex dissolved in DCM to vapour-diffusion of pentane at room temperature. ^{1}H-NMR (300 MHz, $CDCl_3$, **Figure S7**) δ: 8.56 (s, 1H), 8.55 (s, 1H), 7.75 (d, *J* = 7.2 Hz, 1H), 7.72 (d, *J* = 8.0 Hz, 1H), 7.56 (t, *J* = 7.9 Hz, 1H), 7.43 (s, 1H), 7.41 (d, *J* = 2.6 Hz, 1H), 7.35 (t, *J* = 7.3 Hz, 1H), 6.99 (d, *J* = 2.5 Hz, 1H), 3.52 (m, 1H), 3.24 (m, 1H), 2.81-2.76 (m, 2H), 1.34 (s, 9H), 1.25 (s, 9H) ppm. ^{13}C-NMR (125 MHz, $CDCl_3$, **Figure S8**) δ: 163.3, 156.7, 144.6, 139.1, 138.2, 133.6, 131.9, 130.4, 127.4, 125.6, 124.4, 120.6, 117.0, 61.3, 47.5, 34.4, 33.9, 31.2, 29.5 ppm.

$L_{tBu}^{NO}Ni$: To a stirring solution of $L_{tBu}^{NHOH}Ni$ (25.3 mg, 0.0496 mmol) in dichloromethane (2 mL), was added Celite-supported silver(II) carbonate (1.57 mmol/g, 0.32 g, 0.496 mmol).[4-6] The suspension quickly became dark teal. The mixture was stirred at room temperature for 10 min before being filtered through a plug of cotton and Celite. The filtrate was then dried under vacuum to give a blue-green solid. Crystals suitable for X-ray diffraction were grown by slow layered diffusion of pentane into dichloromethane solution of the complex inside an inert-atmosphere glovebox. The mixture was left standing in the –30°C freezer for 4 days to obtain teal crystals. Yield: 21.2 mg, 85%. ^{1}H-NMR (500 MHz, $CDCl_3$, **Figure S13**) δ: 8.02 (d, *J* = 8 Hz, 1H), 7.89 (t, *J* = 8 Hz, 1H), 7.52 (s, 1H), 7.45 (t, *J* = 8 Hz, 1H), 7.39 (d, *J* = 2.5 Hz, 1H), 6.99 (d, *J* = 8 Hz, 1H), 6.93 (d, *J* = 2.5 Hz, 1H), 3.66 (t, *J* = 6 Hz, 2H), 3.43 (t, *J* = 6 Hz, 2H), 1.38 (s, 9H), 1.25 (s, 9H) ppm. ^{13}C-NMR (125 MHz, $CDCl_3$, **Figure S14**) δ: 163.8, 161.7, 161.6, 139.8, 139.2, 138.3, 136.2, 131.5, 130.5, 126.0, 125.2, 118.4, 117.2, 62.0, 47.4, 35.4, 33.9, 31.2, 29.2 ppm.

$L_H^{NHOH}Zn$: To a stirring solution of $Zn(NO_3)_2{\cdot}6H_2O$ (150.8 mg, 0.507 mmol) in ACN (5 mL), a solution of L_H^{NHOH} (170 mg, 0.507 mmol) and triethylamine (140 µL, 102.6 mg, 1.013 mmol) in ACN (5 mL) was added dropwise. The mixture was stirred vigorously for 30 min, during which a colourless solid precipitated out. The solid was collected by filtration, washed with acetonitrile (10 mL) following by diethyl ether (20 mL) and then dried under vacuum to give a colourless powder. Crystals suitable for X-ray diffraction were grown by slow layered diffusion of pentane into dichloromethane solution of the complex at room temperature. Yield: 112 mg, 55%. ^{1}H-NMR (500 MHz, DMSO-d_6, **Figure S9**) δ: 9.57 (s, 1H), 8.70 (br, 1H), 8.29 (s, 1H), 7.60 (d, *J* = 7.5 Hz, 1H), 7.52 (d, *J* = 7.9 Hz, 1H), 7.41 (t, *J* = 7.5 Hz 1H), 7.18-7.14 (m, 1H), 7.13-7.12 (m, 1H), 7.12-7.09 (m, 1H), 6.66 (d, *J* = 8.3 Hz, 1H), 6.51 (t, *J* = 7.2 Hz, 1H), 3.47 (m, 2H), 2.77 (m, 2H) ppm. ^{13}C-NMR (125 MHz, DMSO-d_6, **Figure S10**) δ: 168.52, 169.49, 145.0, 135.2, 133.7, 131.73, 131.65, 127.6, 122.8, 122.5, 119.7, 116.6, 114.7, 56.9, 46.6 ppm. Elemental analysis: calculated for $C_{15}H_{15}N_3O_4SZn$: C 45.18, H 3.79, N 10.54, S 8.04; found: C 43.00, H 3.89, N 10.51, S 8.45%.

$L_{tBu}^{NHOH}Zn$: To a stirring solution of $Zn(NO_3)_2{\cdot}6H_2O$ (66.3 mg, 0.223 mmol) in ACN (5 mL), a solution of L_{tBu}-NHOH (100 mg, 0.223 mmol) and (62 µL, 45.1 mg, 0.446 mmol) in ACN (5 mL) was added dropwise. The mixture was stirred vigorously in air for 30 minutes, during which a colourless solid precipitated out. The solid was collected by filtration, washed with acetonitrile (10 mL) following by diethyl ether (20 mL) and then dried under vacuum to give a colourless powder. Crystals suitable for X-ray diffraction were grown by slow layered diffusion of diethyl ether into an ACN solution of the complex at room temperature. Yield: 69 mg, 61 %. ^{1}H-NMR (500 MHz, $CDCl_3$,**Figure S11**) δ: 9.30 (s, 2H), 8.07 (s, 1H), 8.02 (d, *J* = 8.8 Hz, 1H), 7.77 (d, *J* = 8.1 Hz, 1H), 7.54 (d, *J* = 2.6 Hz, 1H), 7.51 (s, 1H), 7.25 (m, 1H), 6.80 (d, *J* = 2.5 Hz, 1H), 3.23-3.14 (m, 1H), 3.04-2.96 (m, 1H), 1.59 (s, 9H), 1.27 (s, 9H) ppm. ^{13}C-NMR (125 MHz, DMSO-d_6, **Figure S12**) δ: 169.3, 166.7, 145.2, 139.8, 134.7, 131.9, 131.5, 129.4, 127.64, 127.48, 122.3, 119.0, 116.0, 56.6, 46.3, 35.1, 33.9, 31.8, 30.3 ppm.

$L_{tBu}^{NO_2}Cu(OH_2)$): To a stirring methanol (5 mL) solution of $Cu(OAc)_2.H_2O$ (43.1 mg, 0.216 mmol), a solution of $L_{tBu}^{NO_2}$ (100 mg, 0.216 mmol) in DCM (5 mL) was added dropwise. The colour changed immediately to deep green. The solution was stirred for 15 min and then diethyl ether (10 mL) was added. The precipitated green solid was filtered off, washed with diethyl ether, and dried under vacuum. Yield: 82 mg, 70%. MS (ESI, CH_3CN): 523.115 $[M\text{-}L]H^+$ (**Figure S15**).

2. General Procedure for the Oxidation of Alcohols to Aldehydes

In the glovebox, a Radleys® glass reaction tube was charged with 0.5 mmol of alcohol in 4 mL of solvent (DCM or THF). To this solution, L^{I}_{tBu}-NHOH-Cu (0.25 mmol, 5 mol%), 4-(*N,N*-dimethylamino)pyridine (DMAP, 0.1 mmol, 20 mol%) and 100 mg 4 Å MS were added sequentially. After the addition, a cross-shaped stirring bar was added, and the tube was sealed with the Radleys® perfluoroalkoxyalkane cap. The tube was then transferred to Radleys® carrousel (heated to 50 °C when the solvent is THF) and purged with oxygen (+1 atm vs. ambient atmosphere, *i.e.* 2 atm total), and kept under O_2 pressure throughout the course of reaction, with stirring. The reaction was monitored by taking small aliquots using a long-needled syringe. Each aliquot sample was passed over a small Celite-filled Pasteur pipette to remove metal, followed by the addition of known amount of hexamethylbenzene (HMB) as an internal standard (IS) in 1 mL HPLC grade MeOH in a GC vial. The resulting diluted solution was then injected into the GC-FID.

3. NMR Data

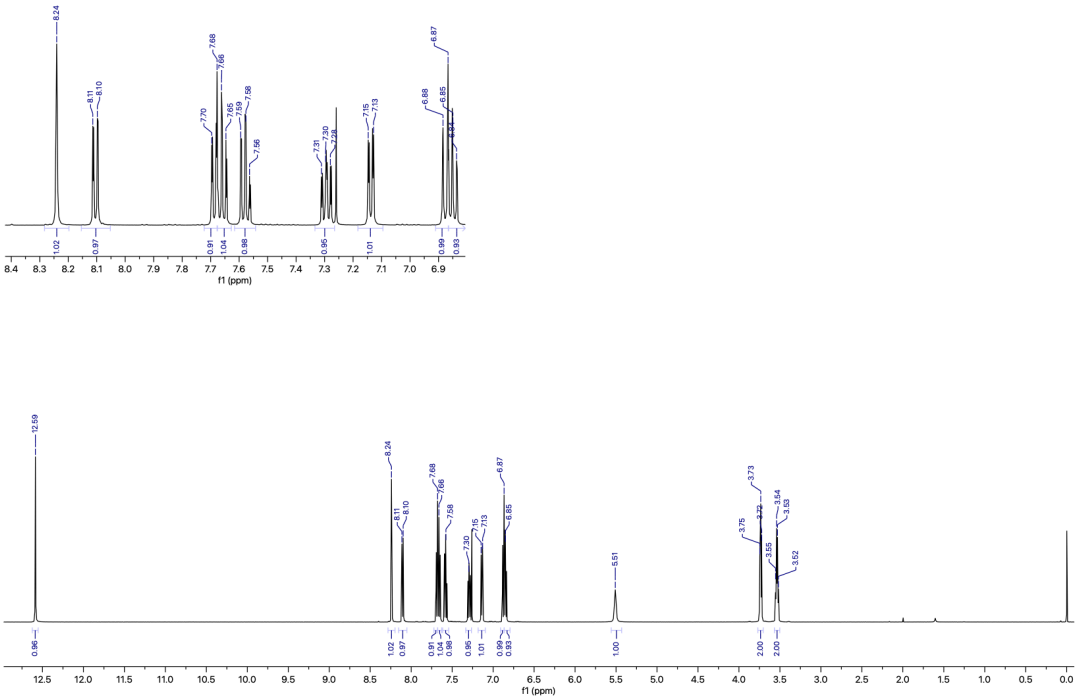

Figure S1. ^{1}H-NMR (500 MHz) spectrum of $\mathbf{H_2L_H^{NO_2}}$ in $CDCl_3$ at 25 °C with inset showing zoom of aromatic region.

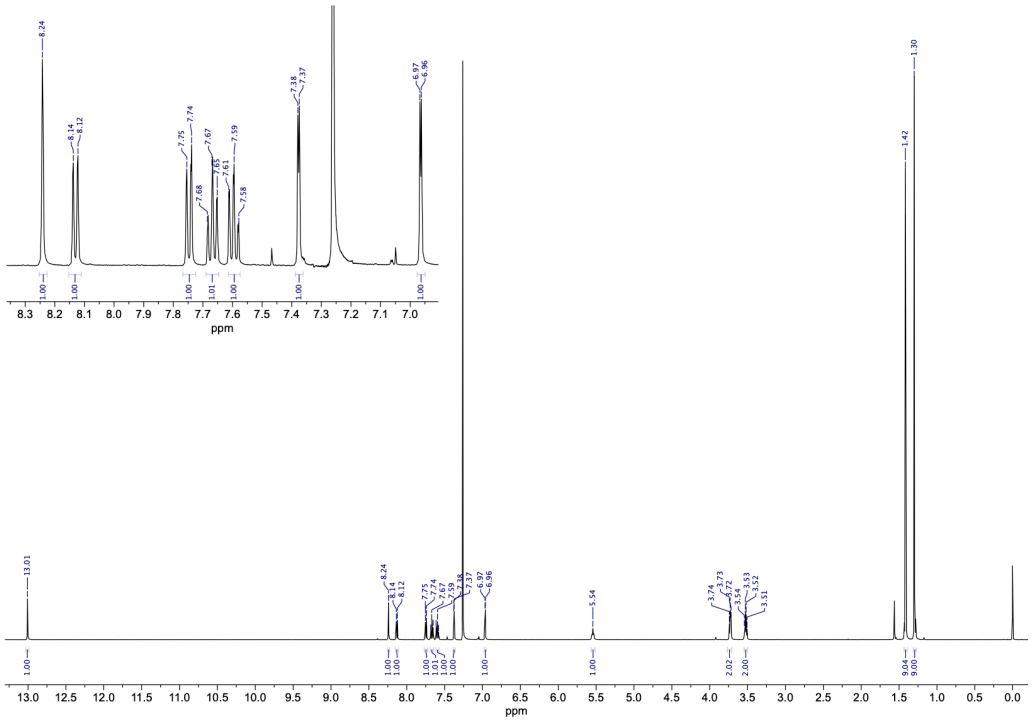

Figure S2. ^{1}H-NMR (500 MHz) spectrum of $\mathbf{H_2L_{tBu}^{NO_2}}$ in $CDCl_3$ at 25 °C with inset showing zoom of aromatic region.

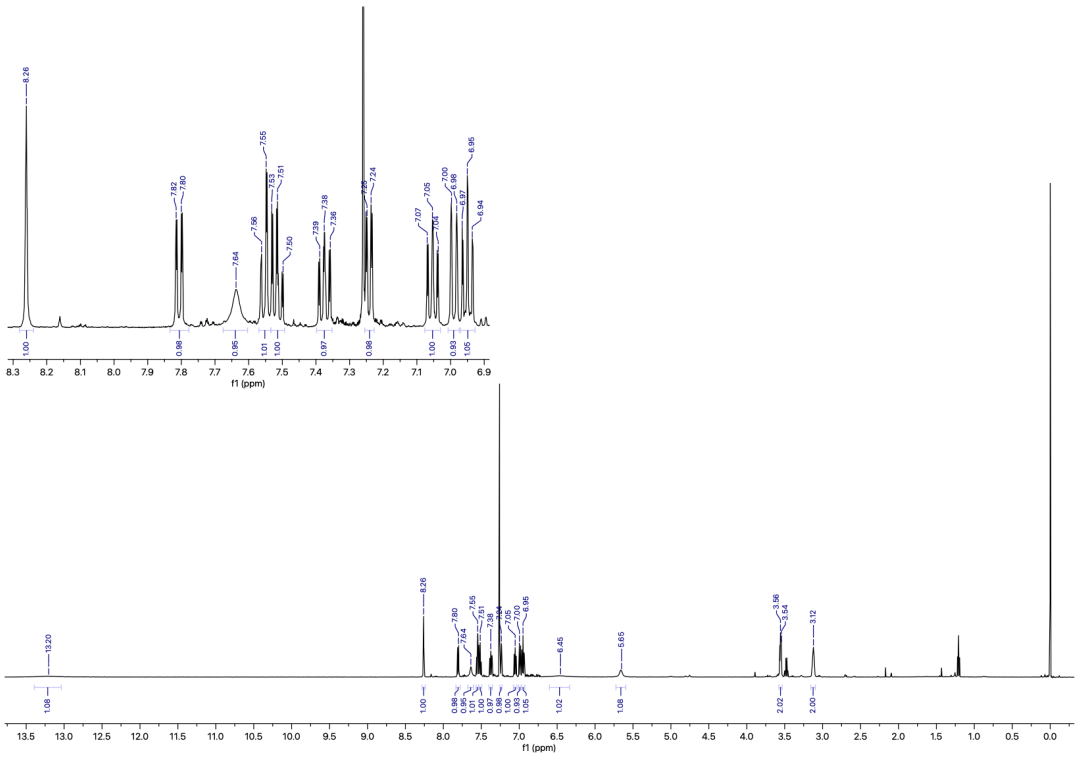

Figure S3. ^{1}H-NMR (500 MHz) spectrum of $\mathbf{H_2L_H^{NHOH}}$ in $CDCl_3$ at 25 °C with inset showing zoom of aromatic region.

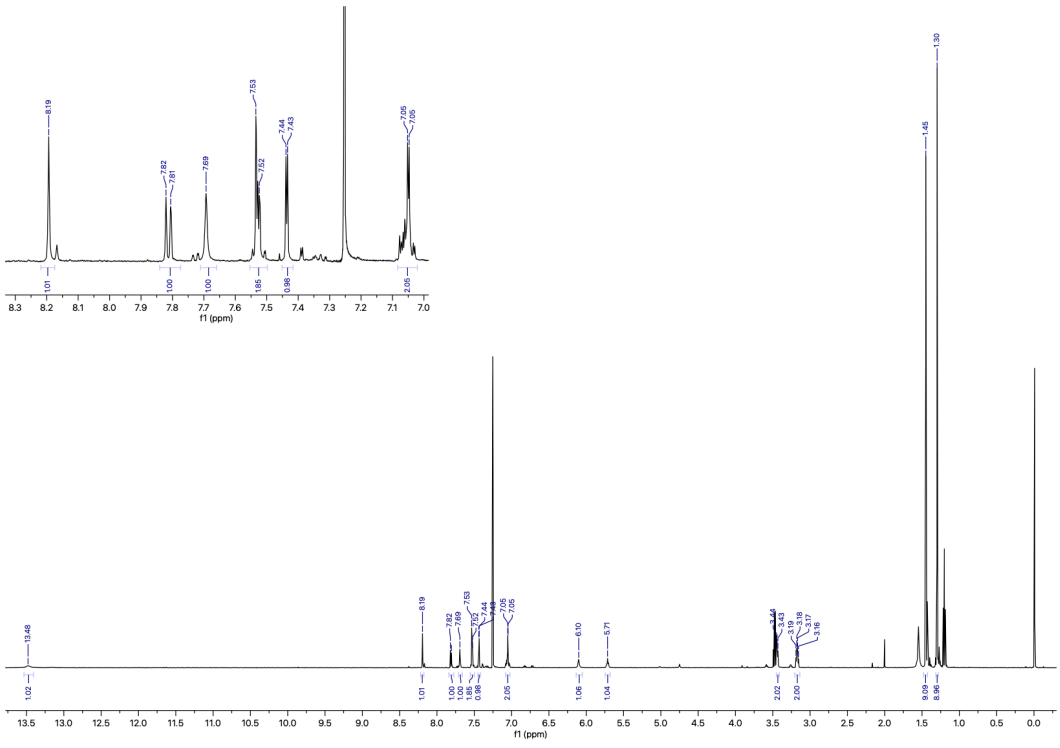

Figure S4. ^{1}H-NMR (500 MHz) spectrum of $\mathbf{H_2L_{tBu}^{NHOH}}$ in $CDCl_3$ at 25 °C with inset showing zoom of aromatic region.

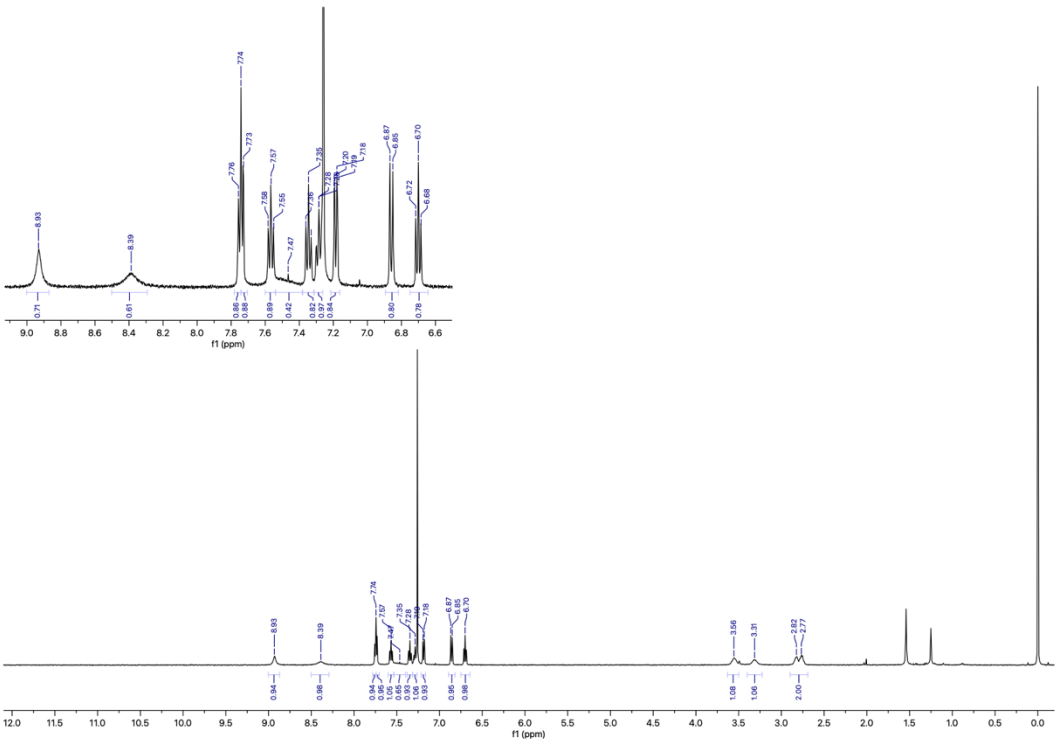

Figure S5. ^{1}H-NMR (500 MHz) spectrum of $\mathbf{L_H^{NHOH}Ni}$ in $CDCl_3$ at 25 °C with inset showing zoom of aromatic region. The CH_2CH_2 region (2.7-3.6 ppm) displays individual signals for each proton, consistent with a rigid ligand backbone.

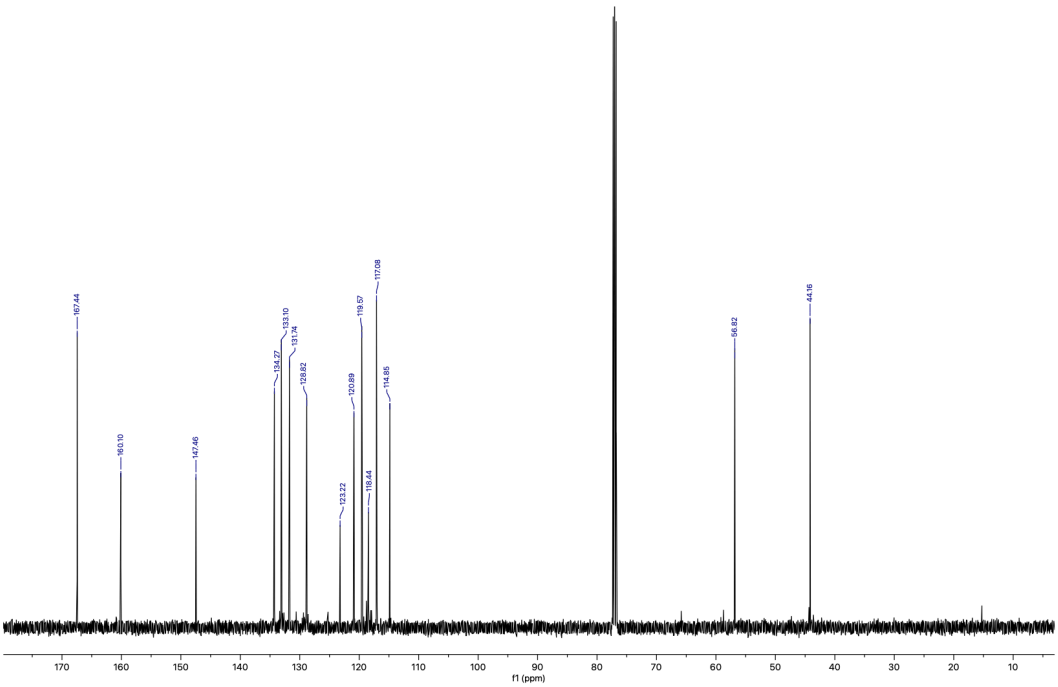

Figure S6. ^{13}C-NMR (125 MHz) spectrum of $\mathbf{L_H^{NHOH}Ni}$ in $CDCl_3$ at 25 °C.

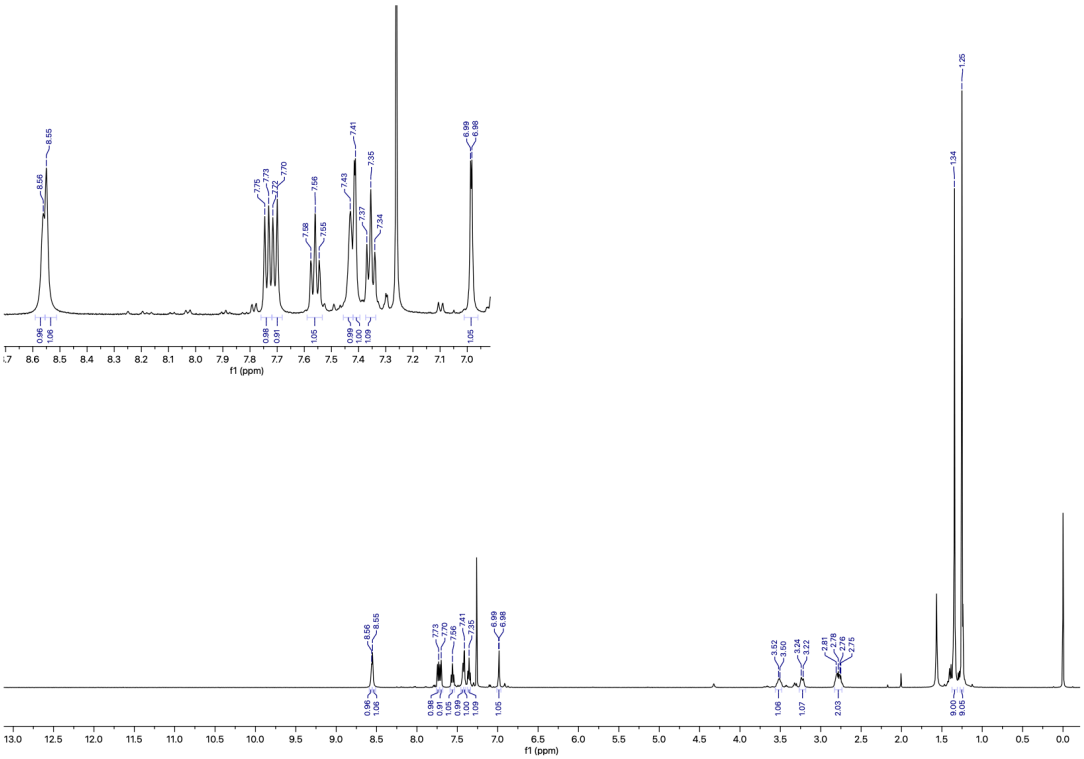

Figure S7. ^{1}H-NMR (500 MHz) spectrum of $\mathbf{L_{tBu}^{NHOH}Ni}$ in $CDCl_3$ at 25 °C with inset showing zoom of aromatic region. The CH_2CH_2 region (2.7-3.6 ppm) showcases a rigid ligand backbone.

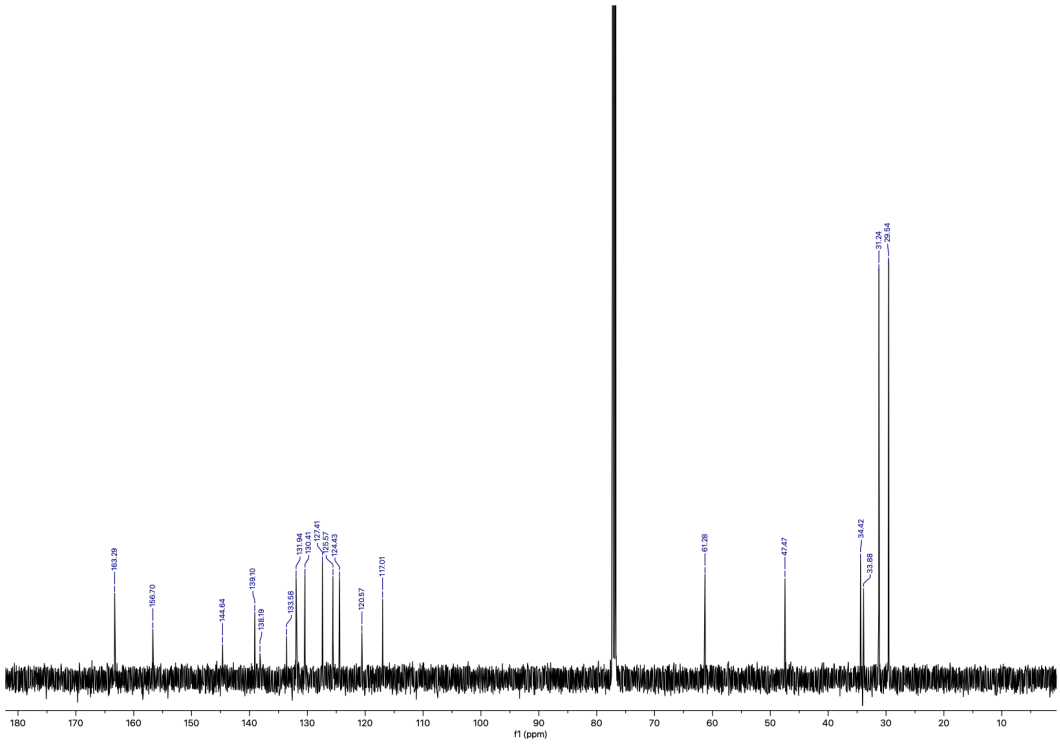

Figure S8. ^{13}C-NMR (125 MHz) spectrum of $\mathbf{L_{tBu}^{NHOH}Ni}$ in $CDCl_3$ at 25 °C.

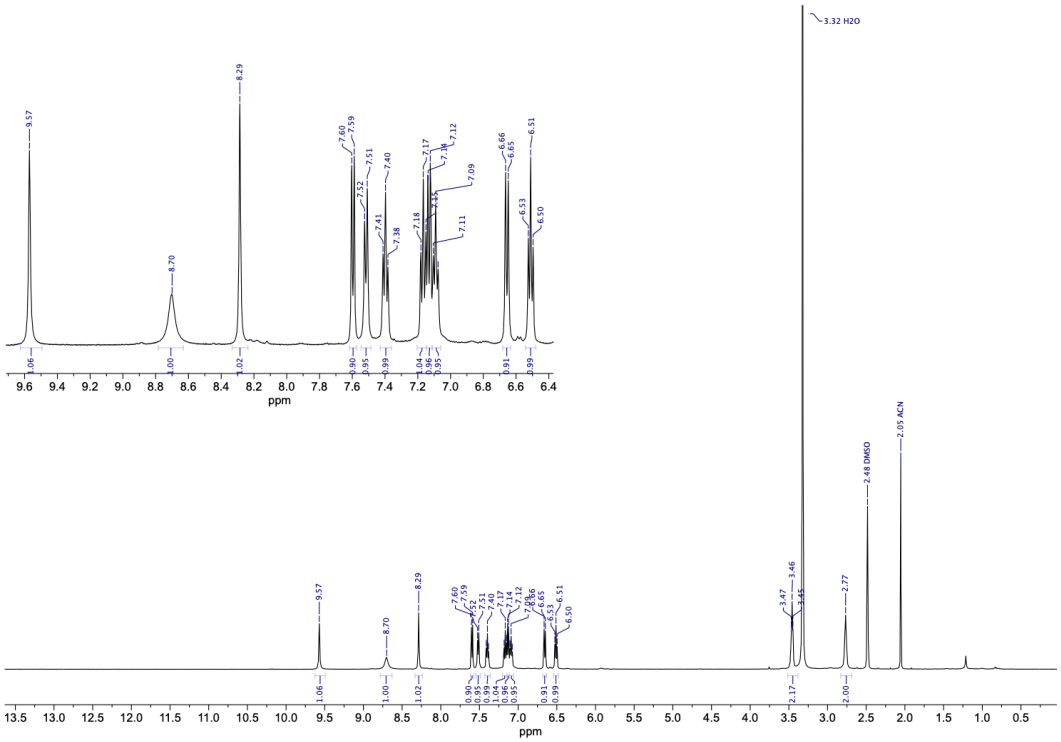

Figure S9. ^{1}H-NMR (500 MHz) spectrum of $\mathbf{L_H^{NHOH}Zn}$ in DMSO-d_6 at 25 °C, inset representing zoom of aromatic region and NHOH proton peaks.

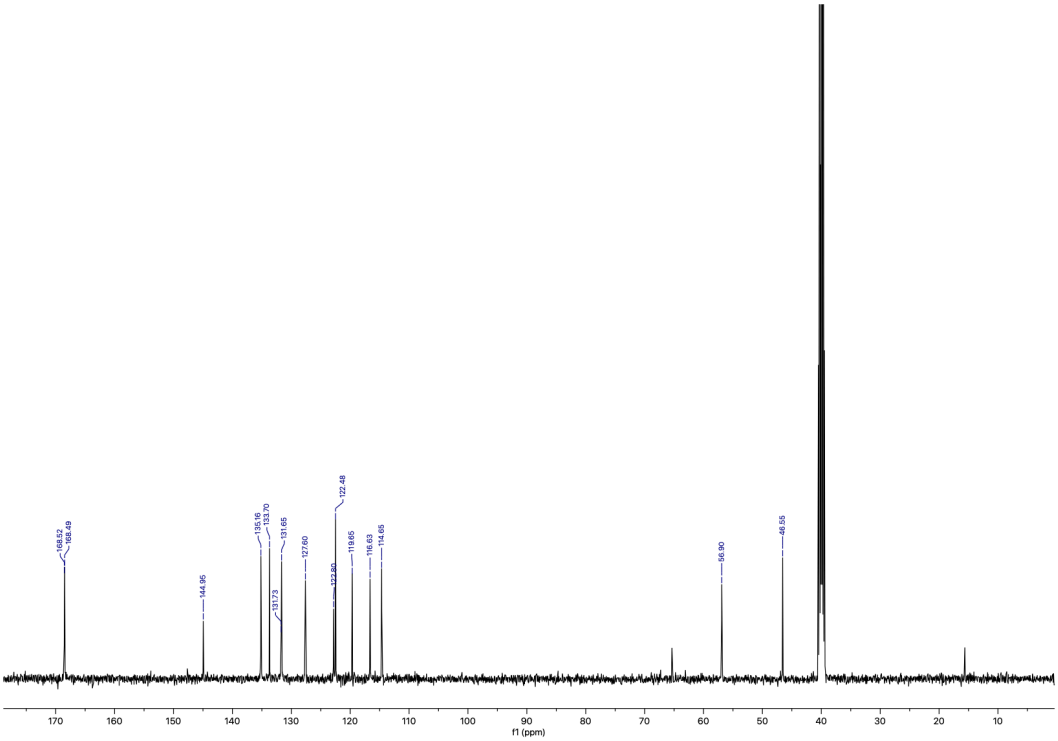

Figure S10. ^{13}C-NMR (125 MHz) spectrum of $\mathbf{L_H^{NHOH}Zn}$ in DMSO-d_6 at 25 °C.

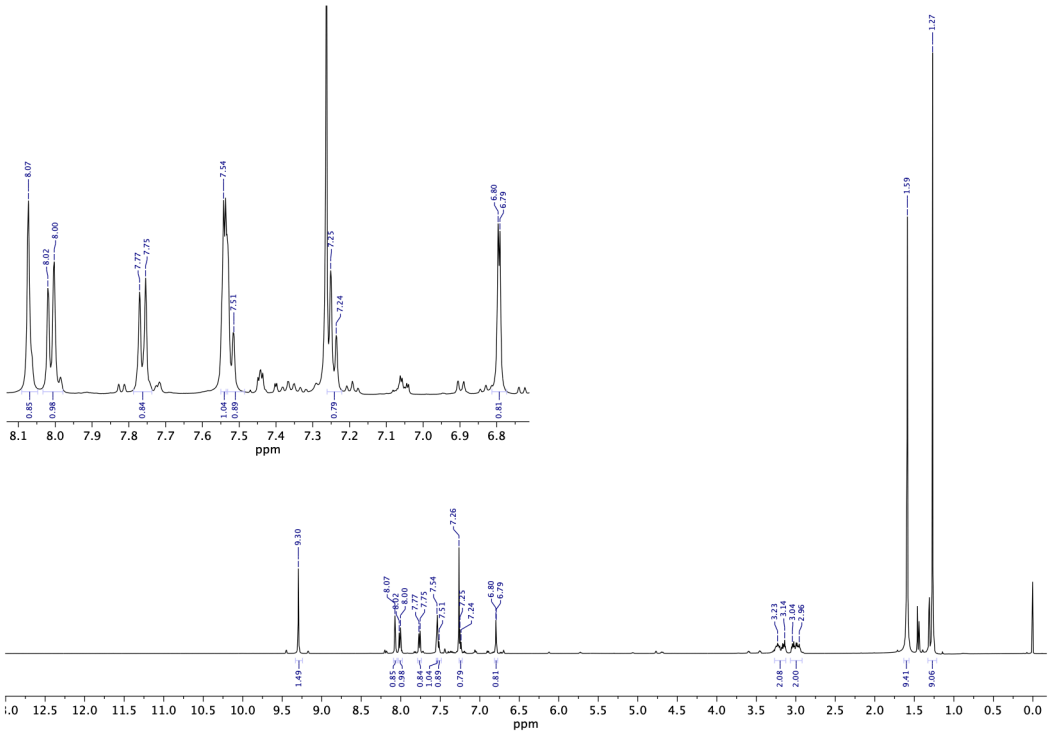

Figure S11. ^{1}H-NMR (500 MHz) spectrum of $\mathbf{L_{tBu}^{NHOH}Zn}$ in $CDCl_3$ at 25 °C, inset representing zoom of aromatic region and NHOH proton peaks.

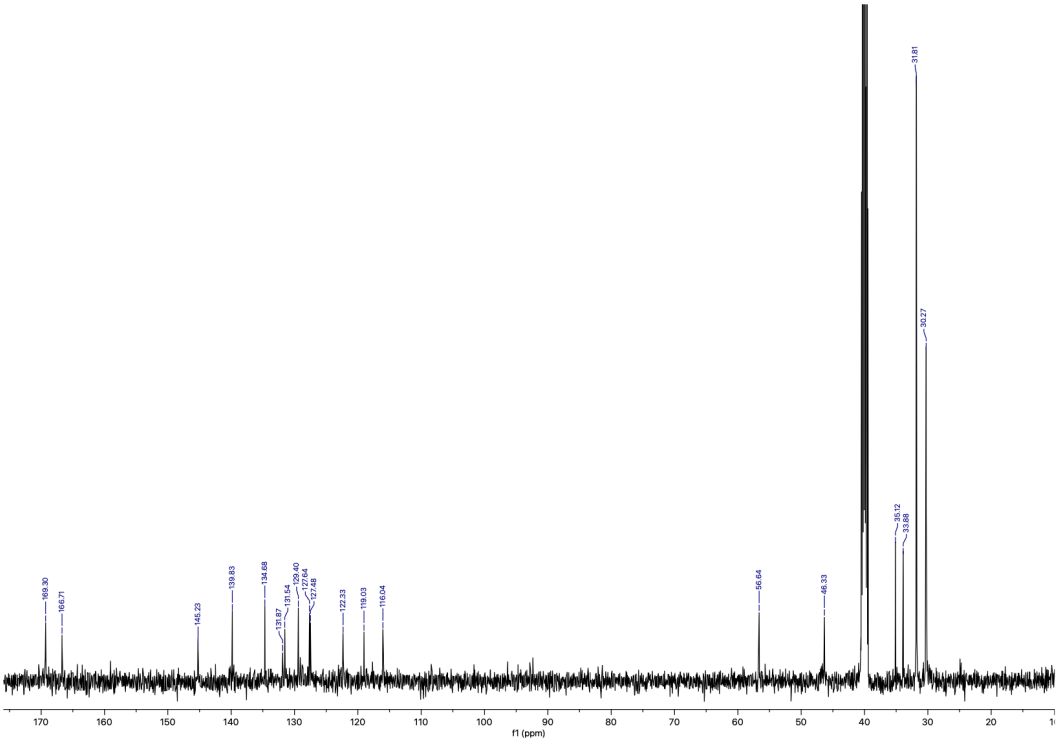

Figure S12. ^{13}C-NMR (125 MHz) spectrum of $\mathbf{L_{tBu}^{NHOH}Zn}$ in DMSO-d_6 at 25 °C.

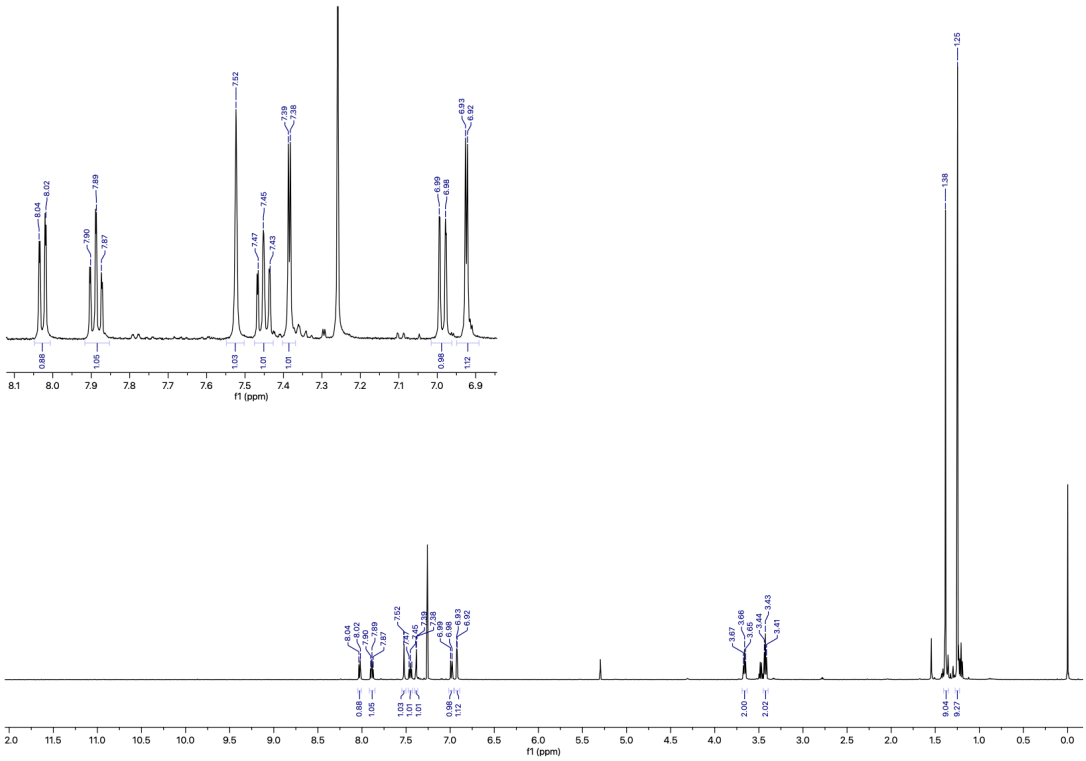

Figure S13. ^{1}H-NMR (500 MHz) spectrum of $\mathbf{L_{tBu}^{NO}Ni}$ in $CDCl_3$ at 25 °C with inset showing zoom of aromatic region.

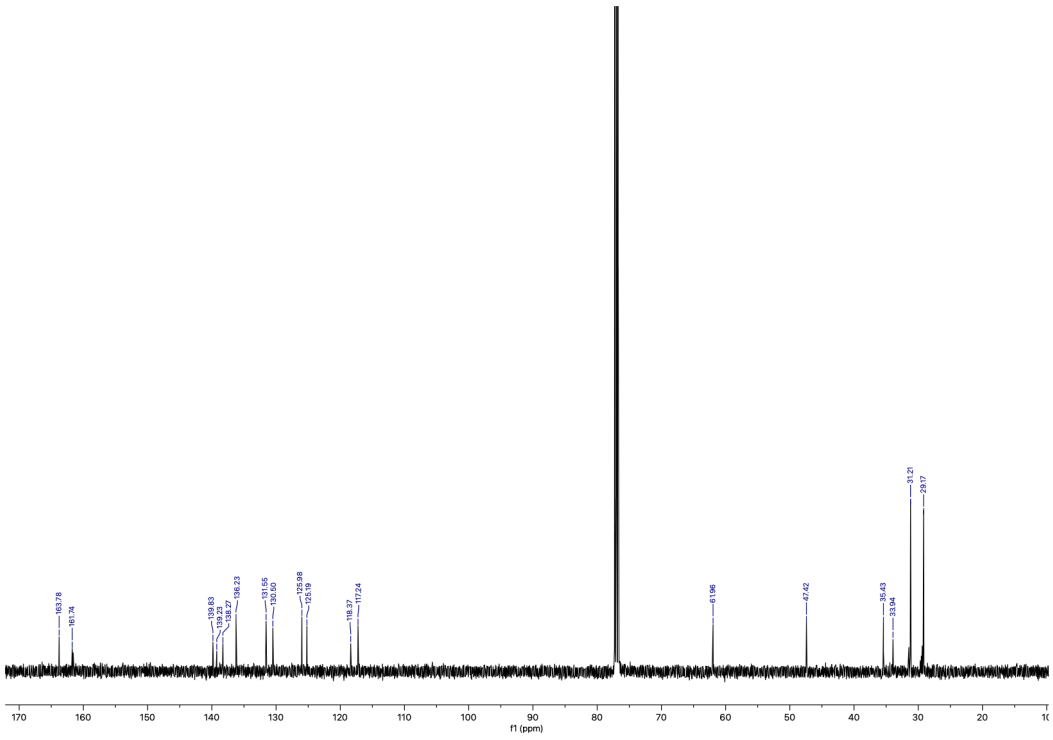

Figure S14. ^{13}C-NMR (125 MHz) spectrum of $\mathbf{L_{tBu}^{NO}Ni}$ in $CDCl_3$ at 25 °C.

4. ESI-MS Data

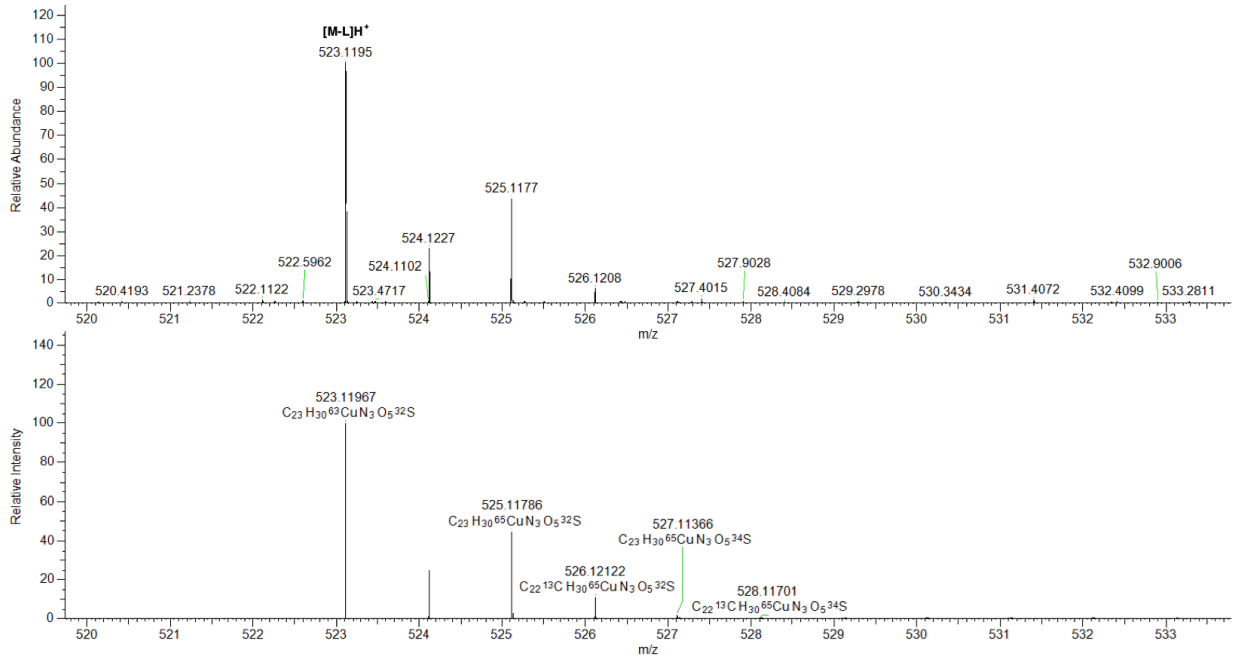

Figure S15. (Top) positive mode ESI-MS of $\mathbf{L_{tBu}^{NO_2}Cu(OH_2)}$ complex in HPLC-grade ACN; (bottom) simulation of isotope splitting pattern expected for $\mathbf{L_{tBu}^{NO_2}Cu(OH_2)}$.

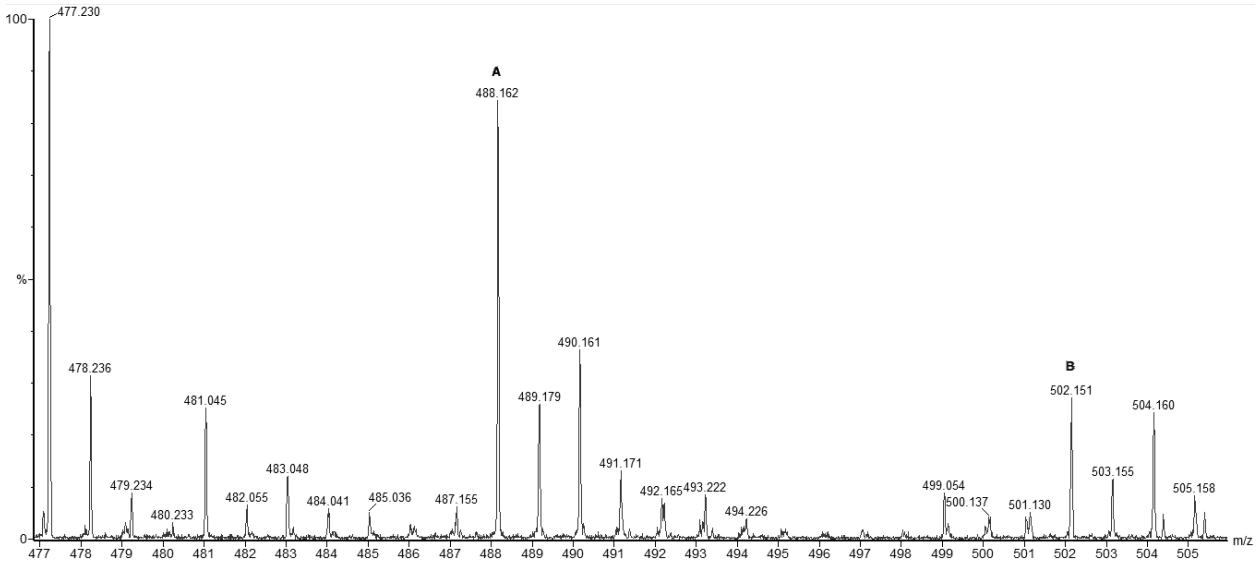

Figure S16. Positive mode ESI-MS showing disproportionation of $\mathbf{L_{tBu}^{NHOH}Ni}$ complex in HPLC-grade ACN. (A) $[L_{tBu}^{NH2}Ni]H^+$, (B) $[L_{tBu}^{NO}Ni]H^+$.

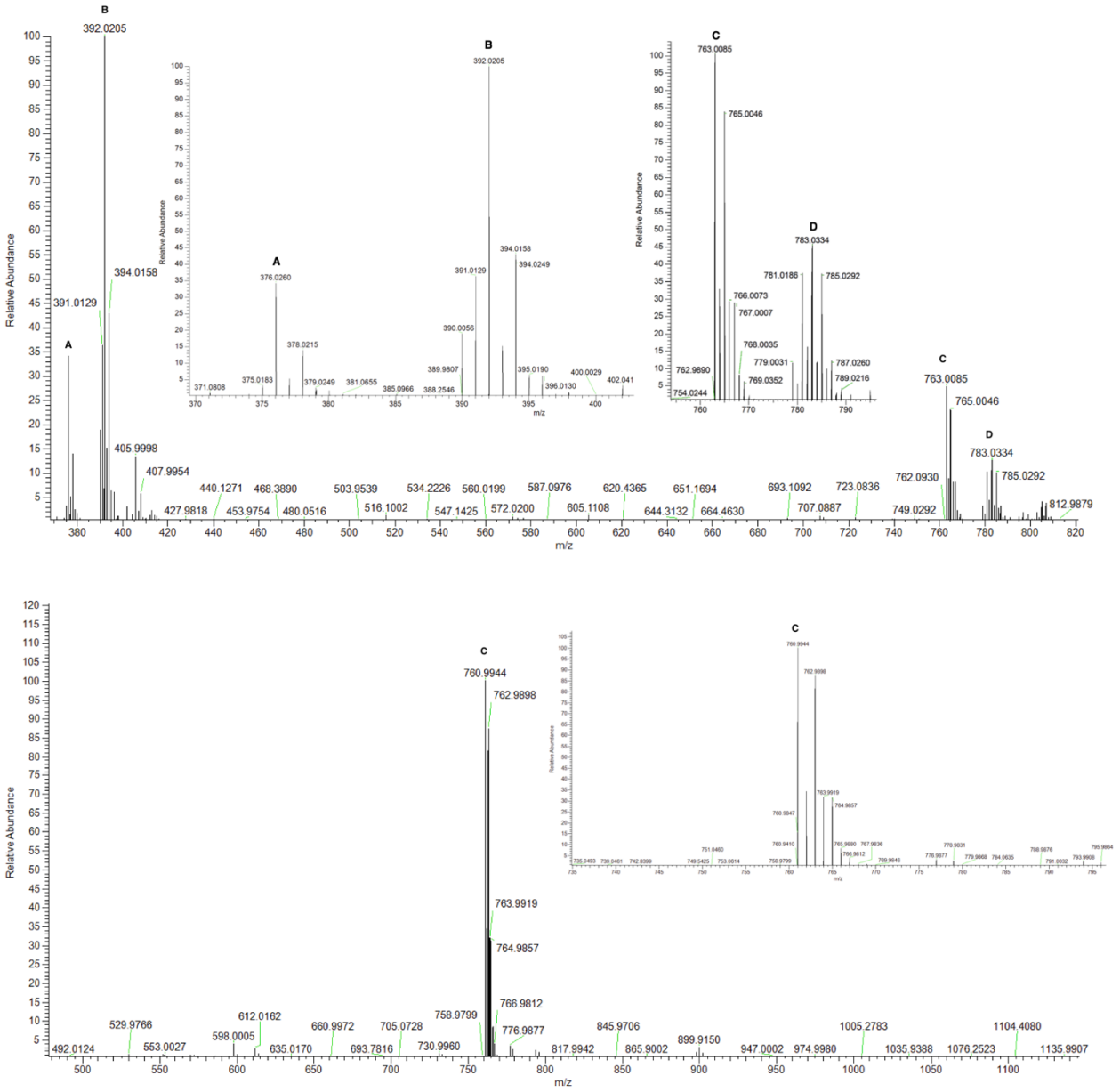

Figure S17. Positive (top) and negative (bottom) mode ESI-MS showing disproportionation and dimerization of $\mathbf{L_H^{NHOH}Ni}$ complex in HPLC-grade ACN. (A) $[L_H^{NH2}Ni]H^+$, (B) $[L_H^{NHOH}Ni]H^+$, (C) protonated ($[(L_H)_2^{N_2O}Ni_2]H^+$, top) and deprotonated ($[(L_H)_2^{N_2O}Ni_2\text{-}H]^-$, bottom) azoxy dimer species, (D) $[L_H^{NHOH}Ni]H^+$ dimer species.

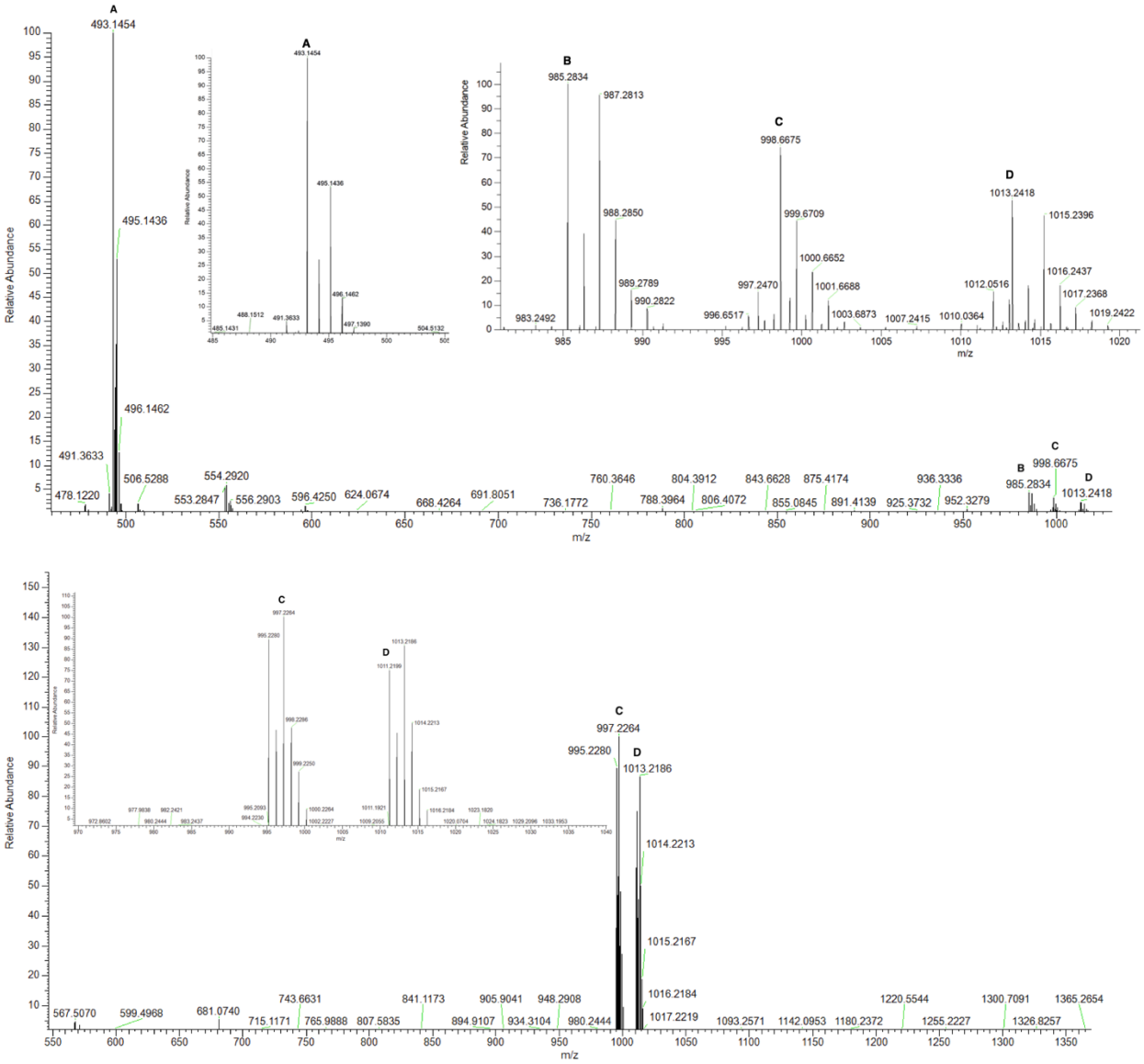

Figure S18. Positive (top) and negative (bottom) mode ESI-MS showing the reactivity of **L_{tBu}^{NHOH}Cu** complex upon oxidation by Fétizon's reagent, in HPLC-grade ACN. (A) $[L_{tBu}^{NH2}Cu]H^+$, (B) protonated azo dimer species, (C) protonated ($[(L_{tBu})_2^{N_2O}Cu_2]H^+$, top) and deprotonated ($[(L_{tBu})_2^{N_2O}Cu_2\text{-}H]^-$, bottom) azoxy dimer species, (D) protonated ($[L_{tBu}^{NO}Cu]_2H^+$, top) and deprotonated $[L_{tBu}^{NO}Cu\text{-}H]_2$, bottom) nitroso dimer species.

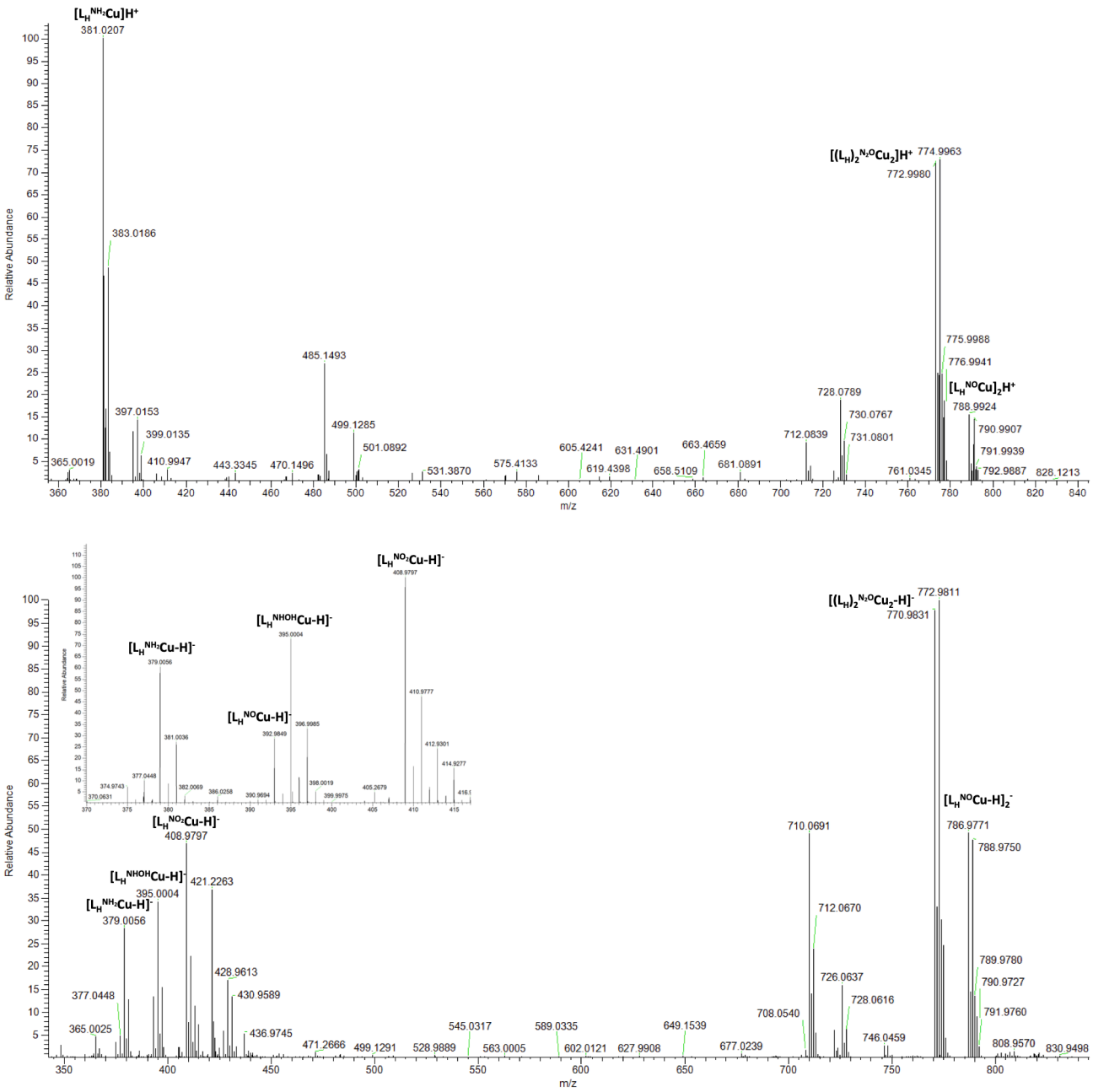

Figure S19. Positive (top) and negative (bottom) mode ESI-MS showing the decomposition products of $\mathbf{L_H^{NHOH}Cu}$ complex after catalysis on 3-methoxybenzylalcohol, in HPLC-grade ACN.

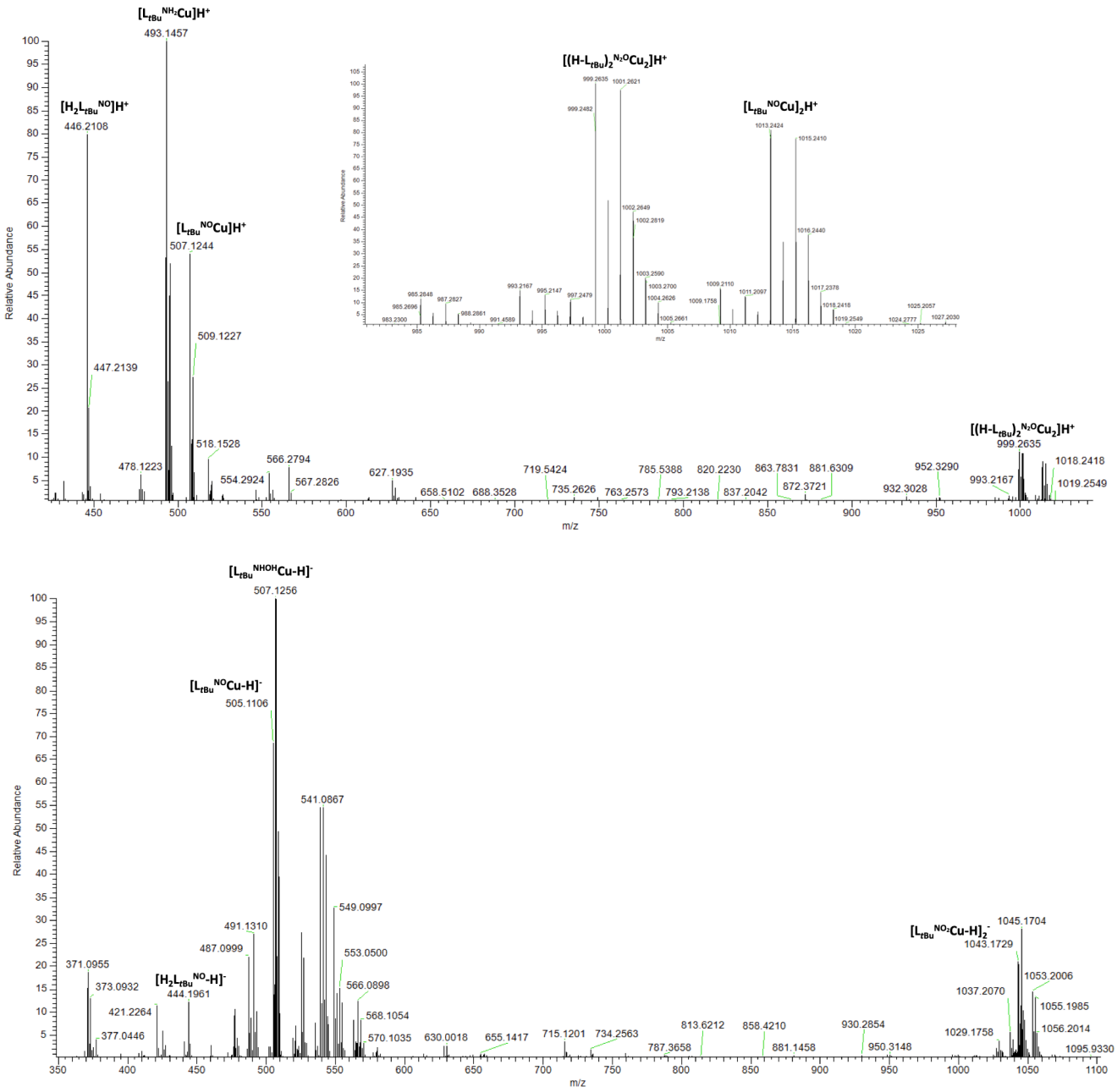

Figure S20. Positive (top) and negative (bottom) mode ESI-MS showing the decomposition products of **L$_{tBu}^{NHOH}$Cu** complex after catalysis on 3-methoxybenzylalcohol, in HPLC-grade ACN.

5. Crystallographic data

Table S3. Crystallographic data for NHOH complexes**.**

	$L_H^{NHOH}Ni$	$L_H^{NHOH}Cu$	$L_H^{NHOH}Zn$	$L_{tBu}^{NHOH}Ni$	$L_{tBu}^{NHOH}Cu$	$L_{tBu}^{NHOH}Zn$
CCDC code	2088565	2088566	2088567	2088568	2088569	2088570
Sample code	Hardeep1	Hardeep5	Hardeep3	Hardeep2b	Fei18	Hardeep6
Formula	$C_{15}H_{15}N_3NiO_4S$	$C_{30}H_{30}Cu_2N_6O_8S_2$	$C_{15}H_{15}N_3O_4SZn$	$C_{23}H_{31}N_3NiO_4S$	$C_{23}H_{31}CuN_3O_4S$	$C_{46}H_{62}N_6O_8S_2Zn_2$, 0.75($C_4O$), 0.25 ($CCl_2$)
F.W. (g mol^{-1})	392.07	793.80	398.73	504.28	509.11	1090.62
T/K	300(2)	150(2)	300(2)	296(2)	110(2)	110(2)
Wavelength/Å	0.71073	0.71073	1.54178	0.71073	1.54178	0.71073
Size/mm^3	0.43×0.12×0.11	0.17×0.15×0.09	0.3×0.1×0.1	0.27×0.20×0.05	0.19×0.15×0.10	0.28×0.10×0.07
Crystal System	Orthorhombic	Monoclinic	Orthorhombic	Monoclinic	Monoclinic	Triclinic
Space Group	Pbcn	$P2_1/c$	Pbcn	$P2_1/c$	$P2_1/c$	P-1
a/Å	14.964(2)	11.2868(12)	15.0116(7)	16.4967(19)	18.1906(3)	12.0902(17)
b/Å	14.964(2)	9.6560(10)	15.0137(9)	12.7673(15)	12.7306(2)	14.849(2)
c/Å	13.6852(19)	14.3063(15)	13.9214(8)	11.5945(14)	10.9264(2)	16.669(2)
α/°	90	90	90	90	90	111.874(2)
β/°	90	94.4720(10)	90	107.073(2)	100.5390(10)	106.757(2)
γ/°	90	90	90	90	90	94.825(2)
V/Å^3	3064.8(7)	1554.4(3)	3137.6(3)	2334.4(5)	2487.62(7)	2596.8(6)
Z	8	2	8	4	4	2
$D_{calc.}$/ g cm^{-3}	1.699	1.696	1.688	1.435	1.359	1.395
μ/mm^{-1}	1.429	1.565	3.660	0.955	2.293	1.088
ϑ_{min}/°	1.361	1.810	2.943	1.291	2.471	1.403
ϑ_{max}/°	27.463	25.341	54.049	25.379	68.494	27.475
Measured Reflections	22491	15265	35142	-	22219	-
Independent reflections	3630	2830	1863	7103	4524	11667
Reflexions with I > 2σ(I)	3248	2329	1610	5748	3562	7302
R_{int}	0.0498	0.0565	0.1057	0.0819	0.0492	0.1056
Parameters	229	218	229	296	293	658
Restraints	0	0	0	0	0	0
Largest Peak	0.512	0.373	0.397	1.121	0.712	0.907
Deepest Hole	-0.523	-0.364	-0.672	-0.675	-0.838	-0.648
Goodness of fit	1.047	1.051	1.202	1.019	1.103	1.027
wR_2 (all data)	0.1016	0.0787	0.1549	0.1654	0.1342	0.1697
wR_2	0.0972	0.0736	0.1498	0.1540	0.1197	0.1509
R_1 (all data)	0.0427	0.0451	0.0912	0.0795	0.0636	0.1231
R_1	0.0365	0.0328	0.0770	0.0627	0.0435	0.0695

Table S4. Crystallographic data for $\mathbf{L_H^{NH_2}Ni{\cdot}0.5H_2O}$, $\mathbf{L_{tBu}^{NO}Ni}$, $\mathbf{(HL_H)_2^{N_2O}Cu}$ and $\mathbf{H_2L_{tBu}^{NO_2}}$.

	$L_H^{NH2}Ni$	$L_{tBu}^{NO}Ni$	$(HL_H)_2^{N2O}Cu$	$H_2L_{tBu}^{NO2}$
CCDC code	2088571	2088572	2088573	2089089
Sample code	Hardeep4	Alyson2	Fei14s	Fed5
Formula	$C_{15}H_{15}N_3NiO_3S$, $0.5(H_2O)$	$C_{23}H_{29}N_3NiO_4S$	$C_{30}H_{28}CuN_6O_7S_2$, CH_2Cl_2	$C_{23}H_{31}N_3O_5S$
F.W. (g mol^{-1})	385.08	502.26	797.17	461.57
T/K	110(2)	110(2)	112(2)	110(2)
Wavelength/Å	1.54178	1.54178	0.71073	1.54178
Size/mm^3	0.04×0.11×0.19	0.03×0.13×0.30	0.23×0.43×0.56	0.1×0.1×0.3
Crystal System	Triclinic	Monoclinic	Monoclinic	Orthorhombic
Space Group	P-1	$P2_1/c$	$P2_1/c$	Pbcn
a/Å	11.9552(9)	16.3521(12)	10.967(2)	19.5284(10)
b/Å	12.1760(9)	12.6368(9)	14.103(3)	7.3377(4)
c/Å	12.7970(9)	11.7356(9)	21.624(4)	34.2044(17)
α/°	98.838(4)	90	90	90
β/°	112.789(4)	106.319(4)	104.421(2)	90
γ/°	108.273(4)	90	90	90
V/Å^3	1548.2(2)	2327.3(3)	3239.2(11)	4901.3(4)
Z	4	4	4	8
$D_{calc.}$/ g cm^{-3}	1.652	1.433	1.635	1.251
μ/mm^{-1}	3.274	2.329	1.027	1.485
ϑ_{min}/°	3.947	2.816	1.741	2.584
ϑ_{max}/°	68.802	68.242	25.525	68.319
Measured Reflections	20646	32384	32350	41231
Independent reflections	5327	4203	6030	4385
Reflexions with I > 2σ(I)	4556	3737	4835	3809
R_{int}	0.0554	0.0751	0.0478	0.0400
Parameters	432	296	495	296
Restraints	0	0	38	0
Largest Peak	0.353	0.743	0.445	0.646
Deepest Hole	-0.425	-0.345	-0.477	-0.342
Goodness of fit	1.097	1.027	1.051	1.108
wR_2 (all data)	0.0953	0.0944	0.0942	0.1246
wR_2	0.0914	0.0907	0.0878	0.1212
R_1 (all data)	0.0461	0.0401	0.0531	0.0527
R_1	0.0375	0.0349	0.0386	0.0460

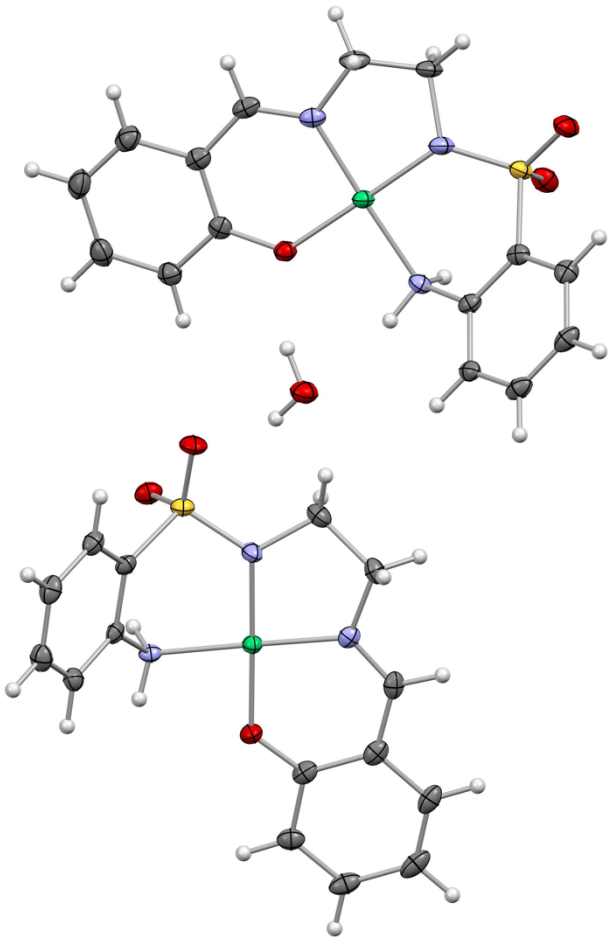

Figure S21. ORTEP at 50% ellipsoid probability for $L_H^{NH_2}Ni \cdot 0.5H_2O$.

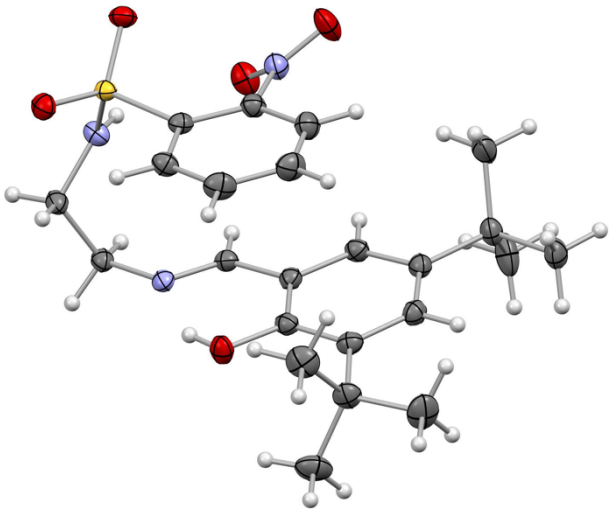

Figure S22. ORTEP at 50% ellipsoid probability for $H_2L_{tBu}^{NO_2}$.

6. References

1. F. Chen, M. S. Askari and X. Ottenwaelder, *Inorg. Chim. Acta*, 2013, **407**, 25-30.

2. J. F. Larrow and E. N. Jacobsen, *Org. Synth.*, 1998, **75**, 1.

3. A. Mori, Y. Miyakawa, E. Ohashi, T. Haga, T. Maegawa and H. Sajiki, *Org. Lett.*, 2006, **8**, 3279-3281.

4. M. Fétizon and M. Golfier, *C. R. Acad. Sci. Ser. C*, 1968, **267**, 900-903.

5. J. A. Maassen and T. J. de Boer, *Recl. Trav. Chim. Pays-Bas*, 1971, **90**, 373-376.

6. M. Fétizon, M. Golfier, P. Mourgues and J.-M. Louis, in *Organic Syntheses by Oxidation with Metal Compounds*, eds. W. J. Mijs and et al., Plenum Press, New York, 1986.